Investigations of the Molecular Mechanism of Metal-Induced Aβ (1−40) Amyloidogenesis[†]

Kwang Hun Lim,*[,‡] Yun Kyung Kim,[§] and Young-Tae Chang[§]

Departments of Chemistry, East Carolina University, Greenville, North Carolina 27858, and New York University, 24 Waverly Place, New York, New York 10003

Received June 6, 2007; Revised Manuscript Received September 14, 2007

ABSTRACT: Transition-metal ions (Cu^{2+} and Zn^{2+}) play critical roles in the Aβ plaque formation. However, precise roles of the metal ions in the Aβ amyloidogenesis have been controversial. In this study, the molecular mechanism of the metal-induced Aβ oligomerization was investigated with extensive metal ion titration NMR experiments. Upon additions of the metal ions, the N-terminal region (1−16) of the Aβ (1−40) peptide was selectively perturbed. In particular, polar residues 4−8 and 13−15 were more strongly affected by the metal ions, suggesting that those regions may be the major binding sites of the metal ions. The NMR signal changes of the N-terminal region were dependent on the peptide concentrations (higher peptide concentrations resulted in stronger signal changes), suggesting that the metal ions facilitate the intermolecular contact between the Aβ peptides. The Aβ (1−40) peptides (>30 μM) were eventually oligomerized even at low temperature (3 °C), where the Aβ peptides are stable as monomeric forms without the metal ions. The real-time oligomerization process was monitored by $^{1}H/^{15}N$ HSQC NMR experiments, which provided the first residue-specific structural transition information. Hydrophobic residues 12−21 initially underwent conformational changes due to the intermolecular interactions. After the initial structural rearrangements, the C-terminal residues (32−40) readjusted their conformations presumably for effective oligomerization. Similar structural changes of the metal-free Aβ (1−40) peptides were also observed in the presence of the preformed oligomers, suggesting that the conformational transitions may be the general molecular mechanism of the Aβ (1−40) amyloidogenesis.

Alzheimer's disease, which affects about 3% of individuals ages 65−74 and nearly half of those age 85 and older, is the most common progressive brain disorder that gradually destroys brain cells and nerves (*1*). Extracellular clumps (or amyloid plaques) deposited in the brain are considered to be the hallmark of Alzheimer's disease (*2*, *3*). Major components of the amyloid plaques in Alzheimer's patients were found to be the 40- and 42-residue β-amyloid (Aβ)[1] peptides, which are the fragments of the amyloid precursor protein (APP) (*2*−*4*). The Aβ (1−40) and (1−42) peptides readily form amyloids under physiological conditions (pH 7.0−7.4, 37 °C) (*3*, *5*, *6*). In addition, amyloids derived from the synthetic Aβ peptides have been shown to be toxic to the cells (*7*−*11*). Thus, elucidating the molecular mechanism of Aβ aggregation is of great importance in developing effective therapeutic agents for Alzheimer's disease.

The Aβ aggregation kinetics is strongly dependent on the experimental conditions, particularly temperature (*3*). For example, the Aβ peptides are highly stable as monomeric forms at low temperatures (<5 °C) (*12*, *13*), while the aggregation propensity is greatly enhanced at higher temperatures (tested up to 85 °C) (*14*, *15*). Transition-metal ions (Zn^{2+} and Cu^{2+}) are also known to play critical roles in the Aβ amyloidogenesis (*16*−*20*). Elevated concentrations of the transition-metal ions (0.5−1.0 mM) have been detected in amyloid plaques found in the brain of Alzheimer's patients (*21*). It was shown that oligomerization of the Aβ peptides is facilitated by the presence of Zn^{2+} ions at physiological conditions (*18*). Trace amounts of Cu^{2+} ions in the drinking water were also able to induce Aβ amyloid formation in rabbits (*22*). In addition, agents that can chelate the metal ions were found to inhibit Aβ aggregation in vitro as well as in vivo (*23*). Thus, detailed characterizations of the effect of the metal ions on the Aβ conformation and aggregation properties would be of great importance in understating the molecular mechanism of Aβ amyloidogenesis.

Extensive biophysical methods including NMR, EPR, and Raman spectroscopy have been used to investigate the metal-coordination geometry and conformational changes of the Aβ peptide upon metal ion binding, and a variety of structural models have been proposed (*24*−*31*). However, detailed understanding of the roles of the metal ions in Aβ amy-

[†] This work was supported by a research development grant (2005) at East Carolina University.

* To whom correspondence should be addressed. E-mail: limk@ecu.edu. Phone: (252) 328-9805. Fax: (252) 328-6210.

[‡] East Carolina University.

[§] New York University.

[1] Abbreviations: NMR, nuclear magnetic resonance; Aβ, β-amyloid; APP, amyloid precursor protein; HFIP, 1,1,1,3,3,3-hexafluoro-2-propanol; $Ru(Bpy)_3Cl_2$, tris(2,2′-bipyridine)ruthenium(II) chloride; APS, ammonium persulfate; SDS, sodium dodecyl sulfate; R_1, spin−lattice relaxation rate; R_2, transverse relaxation rate; HSQC, heteronuclear single-quantum coherence; RDC, residual dipolar coupling; PRE, paramagnetic relaxation enhancement; IPAP, in-phase antiphase; PI3K, phosphatidylinositol 3-kinase; SH3, Src homology 3; TEM, transmission electron microscopy; ThT, thioflavin T; EPR, electron paramagnetic resonance; ICP-AES, inductively coupled plasma atomic emission spectroscopy.

10.1021/bi701112z CCC: $37.00
Published on Web 11/01/2007

loidogenesis is yet to be established. First, the binding site of the metal ions was mapped to the N-terminus (1−16), and the imidazole rings of the three histidines (6, 13, 14) and an oxygen from a side chain (3N1O configuration) were suggested to be responsible for the interactions with the metal ions (*30*, *32*, *33*). However, changes in the structural properties of the Aβ peptides with additions of the metal ions have remained elusive. Second, the molecular mechanism of metal-induced Aβ aggregation is not clearly understood. The Aβ peptides may form monomeric complexes with the metal ions, which may be more amenable to intermolecular interactions. Dimeric complexes bridged by the metal ions were also reported by recent EPR studies, (*27*, *31*) while nonbridged monomeric complexes were suggested by other EPR studies (*29*, *30*). In addition, metal binding to the monomeric Aβ peptides was very recently proposed to inhibit oligomerization, which was probed by electrophoresis, atomic force microscopy (AFM), and thioflavin T (ThT) binding experiments (*26*, *34*, *35*).

In this study, we systematically investigated the effect of the metal ions on the metal-bound conformations and aggregation propensity of the Aβ (1−40) peptide at physiological pH. Extensive metal ion binding studies showed that the metal ions induce subtle conformational changes of the N-terminal region including residue F20 and subsequently facilitate intermolecular interactions between the Aβ peptides. These changes lead to oligomerization even at a low temperature of 3 °C, where the Aβ peptide remains as the monomeric form in the absence of the metal ions. Aβ oligomerization was also detected by kinetic $^1H/^{15}N$ HSQC NMR, ThT fluorescence, and photoinduced cross-linking experiments, which provided valuable insight into the molecular mechanism of an early stage of Aβ amyloidogenesis.

EXPERIMENTAL PROCEDURES

Materials. Commercially available HPLC-purified ^{15}N-labeled recombinant Aβ (1−40) peptides (Recombinant Peptides Inc., Athens, GA) were purchased and used without further purification. Monomeric peptide samples were prepared using 1,1,1,3,3,3-hexafluoro-2-propanol (HFIP; 100%), which has successfully produced monomeric forms of the peptides (*36*). A thin peptide film prepared with HFIP was dissolved by using 1% NH_4OH (1 mg/mL). The peptide samples were dialyzed against 5 mM potassium phosphate buffer (pH 7.0−7.2) at 0−4 °C for NMR experiments. The stock solutions of the Zn^{2+} (0.9 M) and Cu^{2+} (0.93 M) ions were prepared by dissolving $ZnSO_4$ and $CuSO_4$, respectively, into deionized 18 MΩ/cm H_2O. The metal ion solutions were diluted to 0.9 mM (Zn^{2+}) and 0.93 mM (Cu^{2+}) using 20 mM potassium phosphate buffer (pH 7.0−7.2) or the deionized water, and the proper amount of the diluted solution was added to the NMR sample for the metal ion titration experiments. The pH of the NMR sample remained unchanged in the presence of the metal ions. The metal ion concentrations were determined with inductively coupled plasma atomic emission spectroscopy (ICP-AES). Standard copper (0.983 mg/mL in 1% HNO_3, Aldrich) and zinc (1.00 mg/mL in 1% HNO_3, Aldrich) ion solutions were used for the ICP-AES analyses.

The photoinduced cross-linking experiments were carried out by using $Ru(Bpy)_3Cl_2$ and APS, as described in previous papers (*37*, *38*). The two chemicals, 1.5 μL of 1 mM $Ru(Bpy)_3Cl_2$ and 1.5 μL of 20 mM APS in 10 mM sodium phosphate buffer (pH 7.4), were added to 80 μL of the peptide samples. A 200 W incandescent lamp was used to irradiate the mixtures for 15 s to initiate the cross-linking reactions, which were then quenched immediately with 40 μL of Laemmli sample buffer containing 5% μ-mercaptoethanol. A 20 μL portion of each sample was loaded onto an 8−16% gradient SDS gel, and the silver stain was used to stain the gels.

NMR Spectroscopy. All NMR spectra were acquired on a 500 MHz Varian Inova spectrometer equipped with a triple-resonance probe. Peptide concentrations of 15−130 μM (pH 7.0−7.2) were used for the NMR experiments. The HSQC NMR spectrum at 3 °C was identical to the previously reported data for the monomeric Aβ samples (*12*, *39*), and the NMR signal intensity and the chemical shift were not changed before and after the dynamics experiments. The spin−lattice relaxation time (T_1) was measured using eight relaxation delays ranging from 10 to 1300 ms. The T_2 experiments, using the Carr−Purcell−Meiboom−Gill pulse sequence with a 590 μs delay between the π-pulses, were carried out using nine relaxation delays ranging from 10 to 490 ms. All of the relaxation NMR experiments were performed in an interleaved fashion to ensure the experimental conditions were identical for each relaxation delay.

Thioflavin T Binding Assay. Aβ (1−40) peptide (100 μM, pH 7.2) was incubated in the presence and absence of metal ions with various concentrations (0.3−1.8 molar equiv). Following incubation, 50 μL aliquots of the peptide samples were mixed with 150 μL of thioflavin T solution (10 μM thioflavin T in 50 mM glycine buffer, pH 8.5), and fluorescence was measured at 490 nm (excitation at 450 nm) by using SAFIRE2.

Transmission Electron Microscopy. TEM images of Aβ aggregates were obtained using 400 mesh Formvar/carbon-coated copper grids. Aliquots (5 μL) of the peptide samples were adsorbed onto the film for 2 min and negatively stained with a 5 μL drop of 1% uranyl acetate. Images were recorded using a JEOL 1200EX electron microscope.

RESULTS

Zn^{2+} Ion Titration NMR Experiments. Initial metal ion titration experiments were carried out using a peptide concentration of 50 μM at 3 °C (Figure 1). The histidine residues were most significantly perturbed by the Zn^{2+} ions (Figure 1A), as was observed in the previous ^1H NMR studies (*24*, *26*, *28*, *30*, *31*, *40*). The chemical shift changes were accompanied by significant decreases in the NMR signal intensity (Figure 1B). The changes in the NMR signals may originate from the conformational exchanges on the millisecond time scale or deprotonations that were recently proposed (*26*). Thus, the transverse relaxation rates (R_2) were measured with different Zn^{2+} ion concentrations (Figure 1C). The increases in the relaxation rates were correlated well with the NMR signal intensity changes, strongly suggesting that the Aβ (1−40) peptide undergoes conformational fluctuations with metal-bound conformations on the millisecond time scale, as was observed in our and other previous NMR studies (*13*, *41*). However, the enhancement of the relaxation rates was less significant under the less amy-

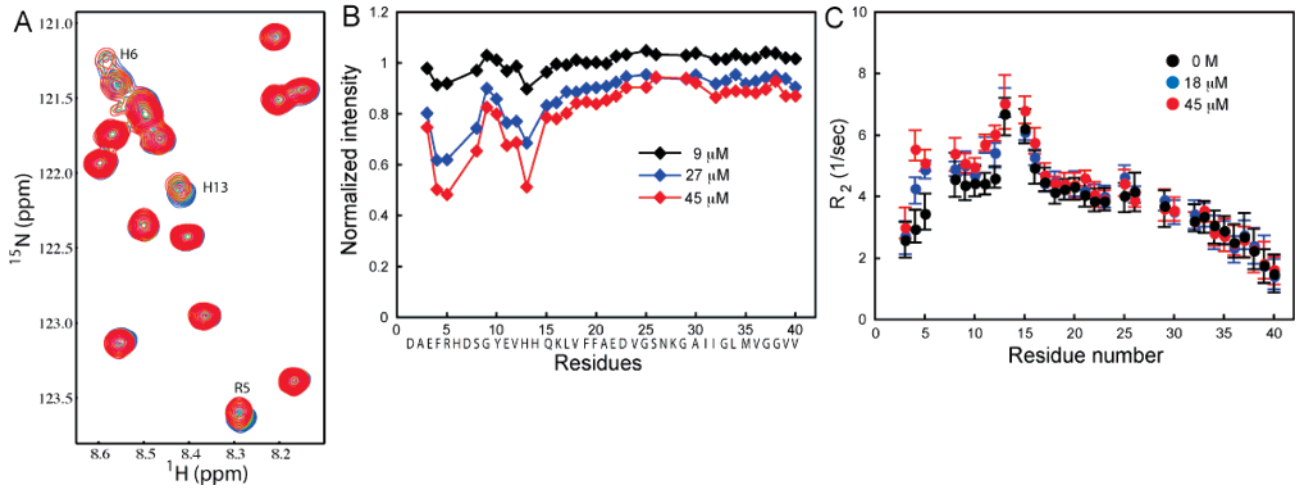

FIGURE 1: (A) ^{1}H/^{15}N HSQC spectra of the Aβ (1−40) peptide (50 μM, pH 7.2) with different Zn^{2+} ion concentrations (blue, 0 M; green, 27 μM; red, 45 μM). (B) Changes in the NMR signal intensities in the presence of Zn^{2+} ions. The maximum signal intensity in the HSQC spectra was used to calculate the intensity ratio. The NMR signal intensity measured at different metal ion concentrations was normalized by that of the HSQC NMR spectrum obtained in the absence of the metal ions. (C) Transverse relaxation rates (R_2) as a function of the Zn^{2+} ion concentrations. The NMR resonance of H6, D7, and H14 was overlapped in the absence of the Zn^{2+} ions.

loidogenic conditions used in the current studies (50 μM and 3 °C) than that in the previous studies (100 μM, 3 °C (*13*); 50 μM, 13 °C (*41*)). This suggests that intermolecular contacts may also contribute to the transverse relaxation rates.

To investigate whether stable dimeric complexes are involved in the conformational exchanges, the titration experiments were repeated with different peptide concentrations (Figure 2A). Interestingly, the extent of the signal changes was considerably reduced at a lower peptide concentration (15 μM). The N-terminal region of the peptide was continuously affected upon addition of Zn^{2+} ions at low peptide concentrations (Figure 2B,C). The effect of the metal ions was consistently more prominent at higher peptide concentrations. At a higher peptide concentration of 80 μM, considerable NMR signal changes were detected even with lower relative concentration of the Zn^{2+} ion (18 μM, 0.23 molar equiv) compared to those at the lower peptide concentrations (Supporting information Figure S1A and Figure 2B). A similar trend was also observed in the chemical shift changes in the metal ion titration NMR spectra (Figure S1). The chemical shift changes for the histidine residues are also more significant at the higher peptide concentrations (Figures S1B−D and 1A). However, the transverse relaxation times of the C-terminal region remained unchanged in the presence of the Zn^{2+} ions (Figure 1C), suggesting that the Aβ peptides do not form stable dimeric complexes. This is consistent with recent pulsed-field-gradient NMR experiments, which showed that the monomeric complexes are dominant before the oligomerization (*41*, *42*). These observations strongly indicate that the changes in the NMR parameters originate from transient intermolecular interactions between the N-terminal residues facilitated by the Zn^{2+} ions. The significant line-broadenings observed in the previous one-dimensional ^{1}H NMR spectra of the Aβ peptides (>1 mM), particularly for the histidine side chains (*24*, *28*, *31*, *40*), may also be due to the intermolecular contacts mediated by the metal ions.

Conformational Changes upon Zn^{2+} Ion Binding. Residual dipolar coupling (RDC) constants were also measured in the presence of Zn^{2+} ions (Supporting Information Figure S2A), to probe conformational changes of the Aβ peptide upon Zn^{2+} ion binding. The overall RDC pattern was not affected by the metal ions, supporting that the Aβ peptides form monomeric complexes with the metal ions. The Zn^{2+} ions appear to induce conformational changes in the N-terminal region (8−10) and residue F20. The higher RDC values upon metal ion binding suggest that those regions adopt a slightly more extended β-sheet-like conformation in the presence of the metal ions. Our previous relaxation NMR measurements showed that the weakly structured N-terminal region is perturbed at stronger amyloidogenic conditions (higher temperature and lower pH) (*13*). In addition, the RDC pattern of the Aβ/Zn^{2+} complex is highly analogous to that of the more amyloidogenic Aβ (1−42) peptide (Figure S2B). In particular, the phenylalanine residue at position 20, which is critical in determining Aβ aggregation propensity, has an extended conformation in the Aβ (1−40)/Zn^{2+} complex that is similar to that found for metal-free Aβ (1−42) peptide. The increased in vivo as well as in vitro neurotoxicity of Aβ (1−42) relative to Aβ (1−40) has been ascribed to differences in the oligomerization rates and/or mechanisms (*43*−*47*). These indicate that the subtle changes in the structural properties induced by metal ion binding may be related to the stronger aggregation propensity of the Aβ (1−40) peptide in the presence of the metal ions.

Cu^{2+} Ion Titration NMR Experiments. The Zn^{2+} ion titration experiments showed that the NMR signal changes are mainly due to the transient intermolecular contact. It is, however, unclear whether the metal ions strongly bind to the Aβ peptides and form monomeric complexes or directly mediate dimeric complexes. Paramagnetic Cu^{2+} ions were, therefore, used for the titration experiments to investigate whether the Aβ peptides form stable monomeric complexes with the metal ions (Figure 3). Almost identical NMR signal changes were observed in the Cu^{2+} ion titration experiments, suggesting that the metal ions selectively interact with the N-terminal region (Figure 3A). However, the decreases in the NMR signal intensities are far more pronounced upon addition of the paramagnetic Cu^{2+} ions. This indicates that the paramagnetic relaxation enhancement (PRE) effect is

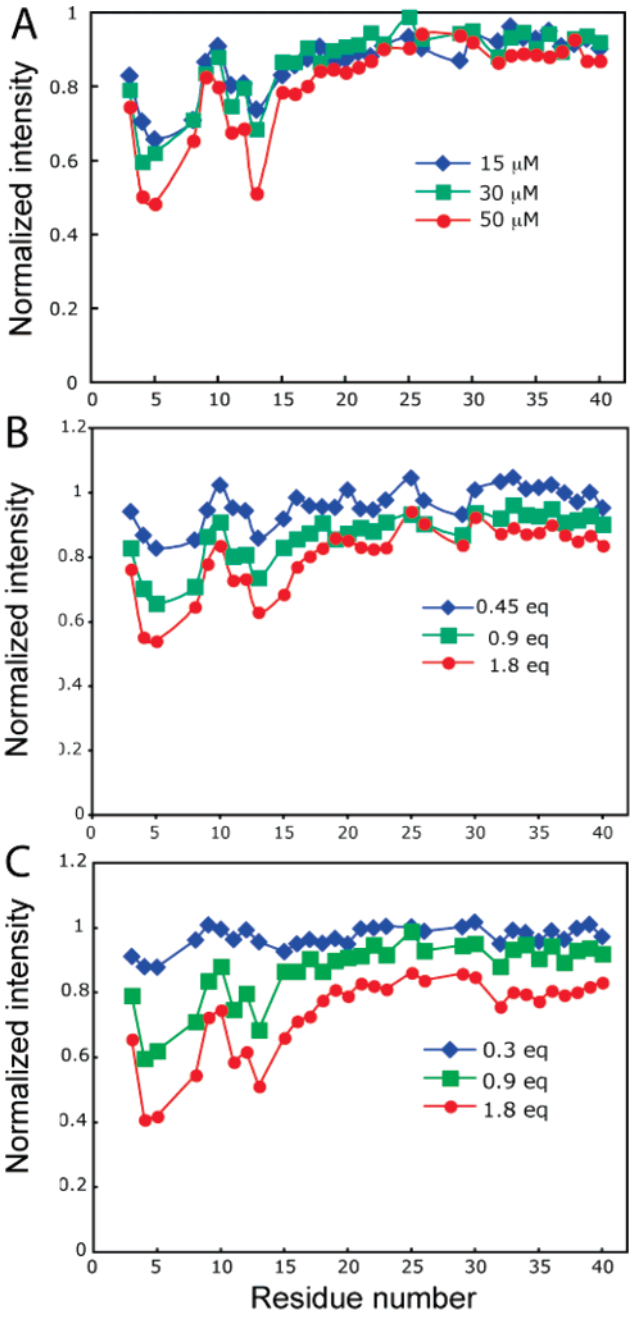

FIGURE 2: (A) NMR signal changes with different concentrations of the Aβ peptide (pH 7.2) in the presence of 0.9 molar equiv of Zn^{2+} ions at 3 °C. (B) Changes in the NMR signal intensity of the Aβ (1−40) peptide (15 μM) as a function of the Zn^{2+} ion concentration (molar equiv) at 3 °C. (C) Changes in the NMR signal intensity of the Aβ (1−40) peptide (30 μM) as a function of the Zn^{2+} ion concentration at 3 °C.

dominant over the conformational fluctuations. Previous Cu^{2+} ion binding studies, however, proposed that the significant NMR signal changes originate from deprotonations and/or chemical exchanges on the millisecond time scale rather than from the PRE by the Cu^{2+} ions (*26*). Thus, spin−lattice relaxation rates, which are insensitive to deprotonation and chemical exchange, were measured (Figure 3B). The relaxation rates are gradually enhanced with higher Cu^{2+} ion concentrations, clearly suggesting the presence of the PRE.

The metal ions are known to interact with the side chains of the three histidines and one additional side chain in the N-terminus. However, the R_1 values of the entire N-terminal

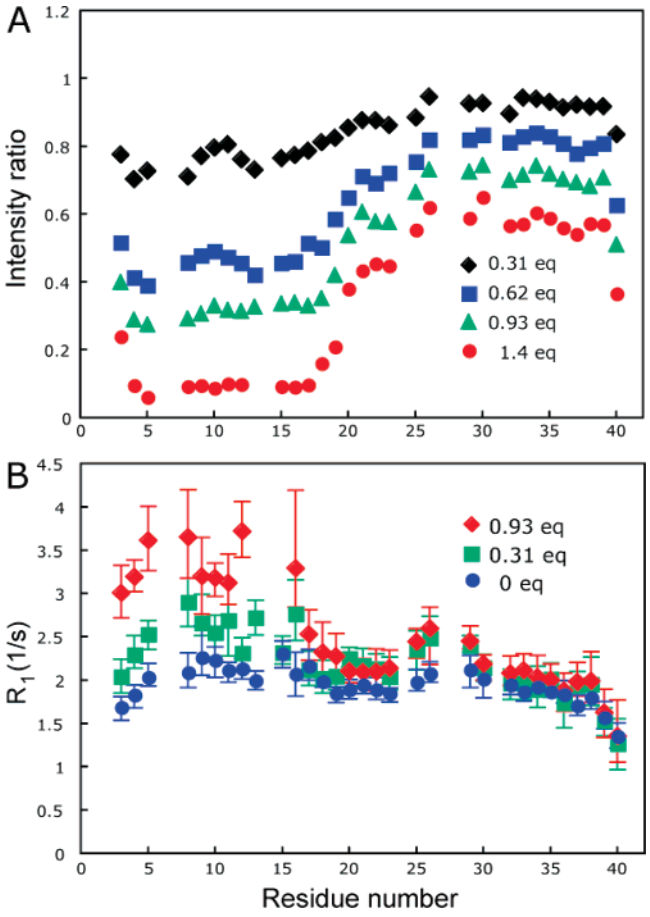

FIGURE 3: (A) NMR signal changes of the Aβ peptide (30 μM, pH 7.2) as a function of the Cu^{2+} ion concentration (molar equiv) at 3 °C. (B) Spin−lattice relaxation rates (R_1) as a function of the Cu^{2+} ion concentration at 3 °C.

region (3−16) are significantly increased, as was demonstrated in other copper binding proteins (*41*, *48*−*50*). This indicates that the Cu^{2+} ions are bound to the N-terminal region strongly enough to induce the PRE. Taken together with the Zn^{2+} ion titration and the RDC experiments, the Aβ (1−40) peptide appears to initially form monomeric complexes with the metal ions bound to the N-terminal region, which may facilitate the intermolecular interactions.

Aβ Oligomerization in the Presence of Metal Ions. The metal ion binding experiments were originally carried out using higher peptide concentrations (Figure S1A). Interestingly, the effect of the Zn^{2+} ions on the NMR signal intensities was saturated at the higher peptide concentration of 80 μM (Figure S1A). In addition, the HSQC NMR spectra gradually changed with new NMR resonances presumably due to oligomerization. The metal ion titration experiments were repeated with a higher Aβ peptide concentration (130 μM) using a Zn^{2+} ion concentration of 40 μM. After 13 h of incubation at 3 °C, new NMR resonances appeared in the HSQC NMR spectrum while certain resonances disappeared (Figure 4A). The NMR spectra continued to slowly change, and the NMR resonances of the monomeric Aβ peptides almost completely disappeared after 5 days of incubation at 3 °C (Figure 4C). The changes in the NMR spectra have not been observed at the lower Aβ peptide concentrations (15 μM) even with the higher Zn^{2+} ion concentration (2 molar equiv). In addition, the Aβ peptides (0.1−0.5 mM) in the absence of the metal ions are highly

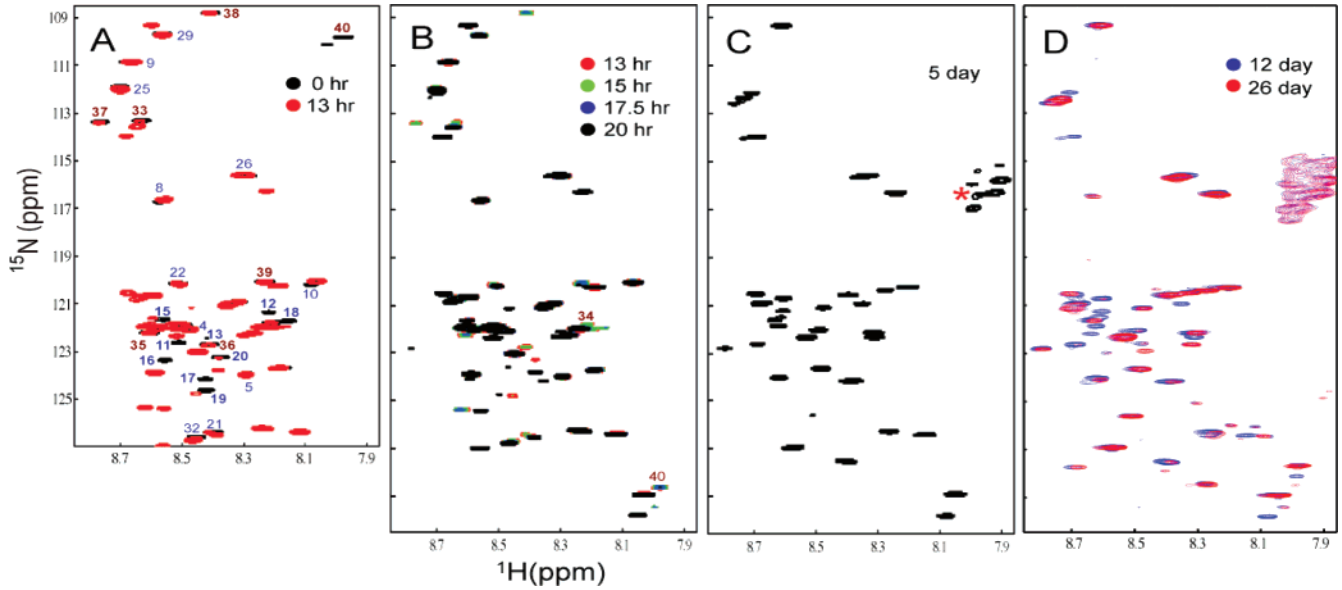

FIGURE 4: Kinetic ^{1}H/^{15}N HSQC NMR spectra of Aβ (1−40) (130 μM) in the presence of Zn^{2+} ions (40 μM) at 3 °C (pH 7.0). The peptide samples were soaked in a 4% polyacrylamide gel after 24 h of incubation to reduce the aggregation rates. The NMR signal intensities gradually decreased with longer incubation times due to oligomerization. Signals denoted with an asterisk originate from the $-NH_2$ group in the gel. Oligomerization was also eventually observed at lower peptide concentrations (>30 μM) with higher relative Zn^{2+} ion concentrations (1.8 molar equiv) after longer incubation (>2 weeks) at 3 °C.

stable in monomeric form at low temperature (*12*), strongly suggesting that the changes in the HSQC spectra are caused by intermolecular Aβ interactions facilitated by the Zn^{2+} ions.

Several interesting observations can be made from the kinetic HSQC spectra: First, the broadened NMR resonances in the N-terminal region caused by the Zn^{2+} ions became narrower as in the HSQC spectra without Zn^{2+} ions and remained almost unchanged for at least 24 h (Figure 5 and Supporting Information Figure S3A). Second, NMR signals of residues 10−21 disappeared or significantly decreased, and distinct new NMR resonances appeared after 13 h of incubation (Figures 5 and S3B). With longer incubations, NMR signals of the C-terminal region (32−40) were gradually decreased, while those of residues 22−30 changed more slowly (Figures 5 and S3C,D). Similar trends were also observed at a peptide concentration of 80 μM but with a slower rate. These suggest that the Aβ peptide initially undergoes conformational changes due to the intermolecular interaction between residues 11−20 facilitated by the Zn^{2+} ions, and the C-terminal region readjusts its conformation during oligomerization. The narrow distinct NMR resonances during the conformational changes indicate that the Aβ peptides are in equilibrium between the two states (presumably monomers and oligomers) on slow time scales (greater than milliseconds), and the equilibrium is gradually shifted to the oligomers.

Similar structural transitions were also observed in the presence of Cu^{2+} ions (Figure 6). The signal changes for residues 10−21 could not be detected, since the NMR resonances for the N-terminal residues were already significantly broadened due to the strong PRE by the 1.4 molar equiv of Cu^{2+} ions (Figure 3A). The C-terminal residues (in blue) more quickly disappeared than residues 23−30 (Figure 6), as was observed in the presence of Zn^{2+} ions. These suggest that the two metal ions accelerate the Aβ oligomerization with a similar molecular mechanism. During the initial conformational changes, NMR signals from the N-terminal residues (4−10) are still unobservable, unlike in the HSQC kinetic spectra in the presence of Zn^{2+} ions (Figure 4B), presumably due to the PRE caused by the paramagnetic Cu^{2+} ions. This indicates that the metal ions remain bound to the N-terminal region during the oligomerization process, which was also suggested by EPR studies of the Aβ (1−40) peptide (*32*).

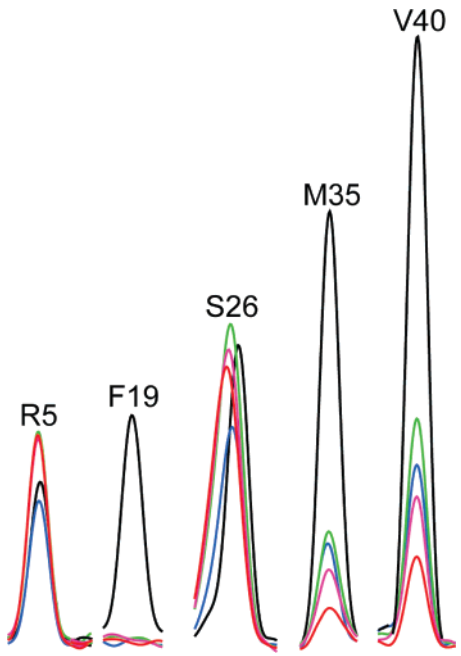

FIGURE 5: 1D slices of the kinetic NMR spectra shown in Figure 4A,B (black, 0 h; blue, 13 h; green, 15 h; magenta, 17.5 h; red, 20 h). NMR resonances of the residues involved in the intermolecular interactions disappeared or were significantly weakened, presumably due to the equilibrium between the monomer and oligomers on the millisecond time scale. The chemical shift of the other residues remained unchanged or slightly changed (Figure S3), suggesting minor structural changes in the equilibrium.

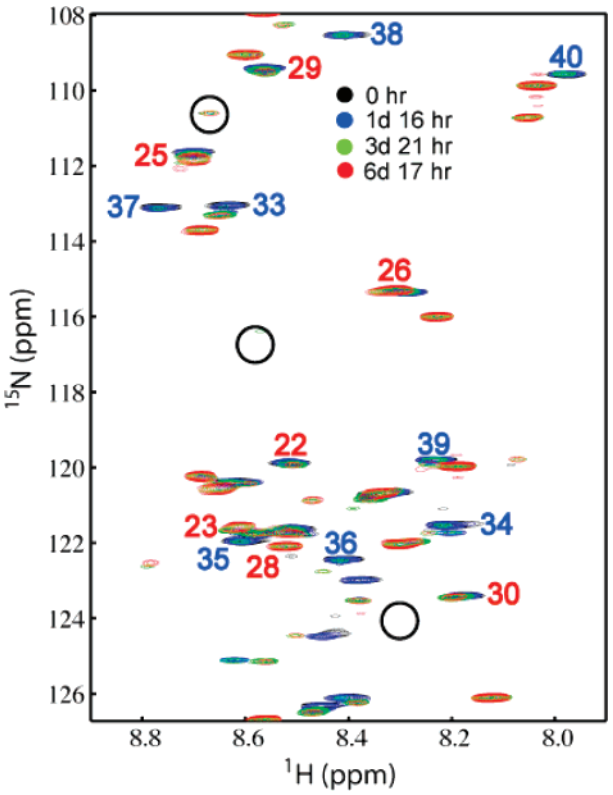

FIGURE 6: Kinetic ^{1}H/^{15}N HSQC NMR spectra of Aβ (1−40) (30 μM) in the presence of Cu^{2+} ions (1.4 molar equiv) at 3 °C (pH 7.0). The circles indicate pick positions for residues G9, S8, and R5 (top to bottom) in the absence of the Cu^{2+} ion.

The conformational changes during the oligomerization process were also detected in the absence of the metal ions (Figure 7). The Aβ peptides were initially incubated at amyloid-forming conditions (100 μM, pH 7.0, 17 °C). After 5 days of aging, the overall NMR signal intensity was decreased by more than 50% due to the Aβ oligomerization (Figure 7A). The temperature of the aged Aβ sample was then lowered to 3 °C, and the HSQC NMR spectra were monitored. The initial HSQC spectrum was identical to that from monomeric Aβ peptides. However, the monomeric forms of the Aβ (1−40) peptide gradually underwent conformational changes (Figure 7B,C), as was observed in the presence of the metal ions (Figure 4A,B). These suggest that the Aβ (1−40) peptide is oligomerized with a common molecular mechanism in the presence and absence of the metal ions. The preformed oligomers induced either by the metal ions or at higher temperatures (>5 °C) appear to initially interact with residues 17−21 of the monomeric Aβ peptides. The hydrophobic residues (Leu-17, Phe-19, and Phe-20), which have a relatively high propensity to form a β-sheet conformation, may play an important role in initiating the intermolecular interactions (*51*−*53*), as also was shown in the amylin peptide (*54*). Further oligomerization was accompanied by the structural rearrangement of the C-terminal region (32−40).

To determine the size distributions of oligomers in the presence of metal ions, photoinduced cross-linking experiments were performed, which were then analyzed by SDS−PAGE electrophoresis (Supporting Information Figure S4). Although monomeric forms of the Aβ (1−40) peptide are predominant over the oligomeric forms at low temperatures (<5 °C), transiently populated small oligomers (<37 kDa) with short lifetimes were detected in the cross-linking experiments, as reported in previous studies (*38*, *55*, *56*). Upon addition of the two metal ions, two bands for the larger oligomers (54−99 kDa) were observed, indicating that the intermolecular association to the oligomers is facilitated by metal ion binding. Big oligomers with the same sizes were also detected for the Aβ sample aged for 2 days without metal ions. These suggest that the Aβ (1−40) oligomerization takes place with a common molecular mechanism, and the oligomerization kinetics depends on the metal ion concentration.

Recently, morphology of the Aβ aggregates was shown to be strongly dependent on the metal ion concentration. ThT fluorescence binding assays were carried out to investigate the degree of the Aβ oligomers observed in the kinetic NMR and cross-linking experiments (Supporting Information Figure S5). The fluorescence intensity for the Aβ oligomers induced by the metal ions at 4 °C remained almost unchanged (Figure S5A), in comparison to that of the Aβ sample incubated at 37 °C (Figure S5B). This indicates that the Aβ oligomers involved in the aggregation process observed in this study are more likely less fibrillar aggregates that are not detected by the ThT binding assay. The TEM images also confirmed that the Aβ peptides formed nonspecific aggregates in the presence of metal ions at 4 °C (Figure S6).

DISCUSSION

Evidence that supports the crucial roles of metal ions in Aβ amyloidogenesis has been growing (*57*, *58*). Therapeutic agents targeting the metal ions have, therefore, been developed and tested for the treatment of Alzheimer's disease (*58*, *59*). However, the precise roles of the metal ions in the Aβ amyloidogenesis are still under debate. Recently, it was proposed that the metal ions may prevent Aβ oligomerization with anomalous binding modes at low temperature (<5 °C), on the basis of the experimental observations that big aggregates were not detected by the AFM and thioflavin T fluorescence binding studies (*26*, *34*, *35*). On the other hand, the metal ions were shown to induce Aβ aggregation, but facilitate the formation of less ordered aggregates (*60*, *61*).

In this study NMR spectroscopy, which is more sensitive to monomers and small oligomers, was utilized to investigate the early stage of oligomerization. The Aβ (1−40) peptide is highly stable in monomeric form at low temperatures (<5 °C). In the presence of metal ions, the Aβ peptides underwent subtle structural changes in the N-terminal region, which was observed by the RDC measurements (Figure S2). Recent NMR and CD studies showed that the N-terminal region (1−16) of the Aβ peptide does not undergo major conformational changes upon metal ion binding (*28*, *41*). However, extensive other CD studies demonstrated noticeable conformational changes of the Aβ peptides due to metal ion binding (*30*, *40*, *62*−*65*). The N-terminal region was shown to adopt a partly structured turnlike structure at low temperatures (<5 °C) (*12*, *66*), which resulted in relatively higher transverse relaxation rates (*13*, *41*). It was demonstrated that the partly structured region was disrupted at stronger amyloidogenic conditions (higher temperatures and lower pH) (*13*). The subtle structural changes caused by metal ion binding may, therefore, result in more facilitated intermolecular interactions

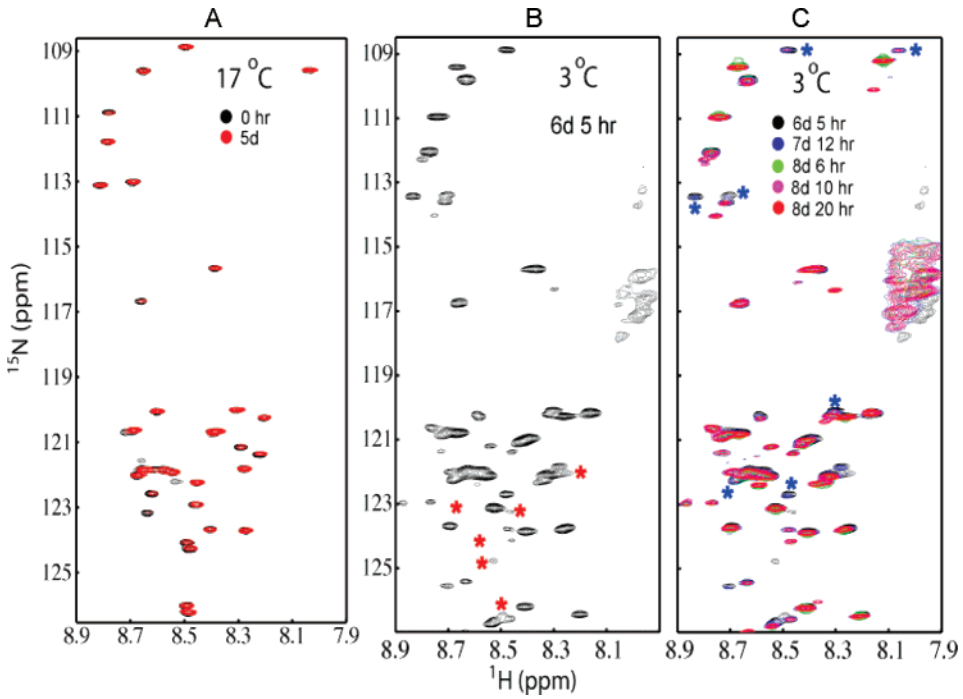

FIGURE 7: Kinetic $^{1}H/^{15}N$ HSQC NMR spectra of Aβ (1−40) (100 μM, pH 7.0) in the absence of the metal ions at (A) 17 °C and (B) 3 °C. The peptide samples were soaked in a 4% polyacrylamide gel after being aged at 17 °C to reduce the aggregation rates. Signals denoted with an asterisk in (B) and (C) indicate weakened NMR signals and/or NMR signals that have disappeared for residues 17−21 and 33−40, respectively.

mainly through the N-terminal region (Figure 2), which can lead to the formation of big oligomers (Figure S4). The large oligomers may then induce oligomerization even at a low temperature of 3 °C, as clearly illustrated in the kinetic HSQC NMR experiments. In the absence of metal ions, almost identical conformational changes during the oligomerization process were observed in the Aβ sample that was aged for 5 days at 17 °C prior to the kinetic NMR experiments (Figure 7). It is well-known that the preformed oligomers accelerate oligomerization (*3*). Thus, the oligomers generated by the metal ions appear to interact with the monomers and induce their conformational changes and subsequent oligomerization.

The real-time kinetic NMR experiments also revealed important residues involved in the intermolecular interactions. Hydrophobic residues 17−21 have been shown to play a critical role in Aβ oligomerization (*51*, *52*, *67*−*70*). It was also shown that the histidine residues in the N-terminus undergo a significant change during the oligomerization process, suggesting their involvement in intermolecular association (*12*). In addition, it was proposed that the more structured C-terminal region in the more amyloidogenic 42-residue Aβ (1−42) peptide may be responsible for the stronger amyloidogenic propensity of the 42-residue peptide than the 40-residue Aβ (1−40) peptide (*12*, *71*). The previous observations are consistent with the kinetic NMR data, which showed that those residues play a crucial role in the oligomerization process. However, interactions between the residues in the N-terminal region (11−21) appear more critical for the initial oligomerization. The initial association of the Aβ peptides through the N-terminal residues may then facilitate hydrophobic interactions between the residues of the C-terminus. This is consistent with previous fluorescence quenching experiments that reported conformational changes of the C-terminal region during the Aβ (1−40) fibrillization

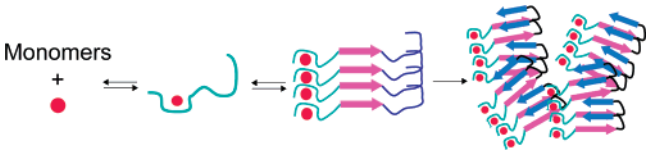

FIGURE 8: Schematic diagram for the proposed molecular mechanism of metal-induced Aβ oligomerization. The Aβ oligomers were drawn on the basis of the structural model derived from extensive solid-state NMR studies (*74*, *82*).

(*72*). However, NMR resonances of residues 22−29 remained almost unchanged in the initial oligomerization (Figure 4A,B). This suggests that those residues may not be involved in the intermolecular association, consistent with EPR, solid-state NMR, and H/D exchange NMR studies (*73*−*75*).

On the basis of our metal ion binding and kinetic NMR experiments, we propose a molecular mechanism of the metal-induced Aβ oligomerization (Figure 8). The Cu^{2+} ion binding experiments showed that the metal ions are strongly bound to the N-terminus and induce the PRE for the entire N-terminal region (Figure 3). In addition, the relaxation times of the C-terminal region and the overall RDC pattern of the Aβ peptide remained unchanged upon metal ion binding (Figures 1C, 3B, and S2). In addition, diffusion NMR experiments showed that the Aβ (1−40) peptide forms monomeric complexes with the metal ions (*41*, *42*). These suggest that the Aβ (1−40) peptides predominantly form monomeric complexes with the metal ions, which may be more amenable to intermolecular interactions. At higher peptide and metal ion concentrations, the formation of the big oligomers (54−99 kDa) was more facilitated in the presence of metal ions due to the intermolecular contact between the N-terminal regions (Figure S4). The oligomeric

complexes can then induce conformational changes of the monomeric Aβ peptides and accelerate amyloid formation. In the absence of metal ions, a similar oligomerization process was observed in the Aβ sample containing the preformed oligomers (Figures S4 and 7). This suggests that the proposed scheme may be the general molecular mechanism of Aβ (1−40) amyloidogenesis. During the oligomerization process, monomeric forms of the Aβ peptides appear dominant over the oligomers (Figures 4, 6, and 7). In addition, the Aβ peptides formed less fibrillar aggregates in the presence of metal ions (Figures S5 and S6). Thus, the small amount of less ordered oligomers may not have been detected in the previous study using electrophoresis, AFM, and ThT binding assays (*26*).

The oligomerization process is also highly correlated with the dynamic properties of the Aβ peptides. Previous ^{15}N relaxation NMR studies of the Aβ peptide have shown that the critical residues (12−21) involved in the initial intermolecular interactions undergo relatively restricted motions on the nanosecond time scale (*13*, *39*, *76*, *77*). On the contrary, the C-terminus of the Aβ peptide was highly flexible on the nanosecond time scale, which may hinder effective intermolecular interactions, as was observed in the kinetic NMR data. This indicates that the flexibility of the polypeptide chain on the nanosecond time scale may play an important role in effective amyloidogenesis, and thus, the dynamics studies would be very useful for identifying the crucial residues, which was demonstrated for the PI3K SH3 domain (*78*) and β_2-microglobulin (*79*).

In addition to the effect of metal ion binding on the aggregation propensity of the Aβ peptide, the detailed nature of the metal-bound conformation still remains controversial, particularly for the metal binding ligand, in addition to the three histidines. Our extensive titration experiments showed that the influence of metal ion binding on residues E3 (*32*), Y10 (*31*), and E11 (*28*), which were proposed to be binding sites by previous studies, is much less significant in comparison to that on the histidines. The COO^- group of residue D7 may be the additional binding site for the metal ions (Figure S7). However, recent EPR studies of various mutant forms of Aβ peptides showed that residue D7 is not directly involved in metal ion coordination (*80*). The coordination of metal ions to the side chains of the H6, H13, and H14 residues appears to affect the neighboring residues such as F4−S8 and E11−Q15 (Figures 1 and 2). Thus, the acidic residues in the N-terminal region may not be directly involved in metal ion binding. However, the D1 residue was not observed in our NMR experiments, and thus, we cannot rule out the potential role of the end residue, which was proposed by ^{13}C NMR and EPR studies (*32*, *41*, *80*).

In summary, the systematic metal ion titration experiments using diamagnetic (Zn^{2+}) and paramagnetic (Cu^{2+}) ions showed that the transition-metal ions not only selectively affect the N-terminal region (4−8 and 13−15), but also facilitate intermolecular interactions between the hydrophobic residues (17−21) (Figure 8). Our photoinduced cross-linking experiments showed that the metal ions (1 molar equiv) induced the formation of big oligomers (54−99 kDa). In addition, the Cu^{2+} ion binding and kinetic experiments demonstrated that the Cu^{2+} ions are strongly bound to the entire N-terminal region even during the oligomerization process. Moreover, the relaxation rates (R_1 and R_2) and RDC pattern of the polypeptide chain, which are strongly sensitive to oligomerization, are not influenced by the metal ions (Figures 1C and 3B) except for the binding sites. These suggest that the Aβ peptides form mainly monomeric complexes with the metal ions bound to the N-terminal region (*29*, *41*, *42*), rather than stable dimeric complexes bridged by the metal ions that was proposed by previous studies with Raman, EPR, and X-ray absorption spectroscopy (*25*, *27*, *81*). Our extensive biophysical studies are also in good agreement with a recently proposed model, which suggested that the metal ions induce a conformational change of the peptide rather than being directly involved in forming metal-bridged oligomers (*42*).

Finally, at higher peptide concentrations (>30 μM), the Aβ (1−40) peptide was slowly oligomerized at 3 °C in the presence of metal ions (>0.2 molar equiv) mainly through residues 12−21 undergoing relatively restricted motions on the nanosecond time scale. The more flexible hydrophobic C-terminal residues were then involved after the critical residues in the N-terminus initiated the intermolecular association. Thus, small molecules that can prevent the intermolecular interactions between those residues may be effective therapeutic agents. In addition, destabilizations of the metal-bound complexes might also be an effective therapeutic strategy for the treatment of Alzheimer's disease.

ACKNOWLEDGMENT

We acknowledge the technical assistance of Dr. Randall Renegar, Director of the Brody School of Medicine Electron Microscopy Laboratory, with β-amyloid sample preparation and photography. Mr. Nagchowdhuri and Mr. Millard are acknowledged for ICP analyses. We also thank Profs. Burns, Love, and Rodriguez for critical reading of the manuscript.

SUPPORTING INFORMATION AVAILABLE

RDC profiles, metal ion titration HSQC NMR spectra, SDS−PAGE of the cross-linked Aβ (1−40) peptides, ThT binding assays, and TEM images. This material is available free of charge via the Internet at http://pubs.acs.org.

REFERENCES

1. Conway, K. A., Baxter, E. W., Felsenstein, K. M., and Reitz, A. B. (2003) Emerging beta-amyloid therapies for the treatment of Alzheimer's disease, *Curr. Pharm. Des. 9*, 427−447.
2. Selkoe, D. J. (1991) The molecular pathology of Alzheimers-disease, *Neuron 6*, 487−498.
3. Harper, J. D., and Lansbury, P. T. (1997) Models of amyloid seeding in Alzheimier's disease and scrapie: Mechanistic truths and physiological consequences of the time-dependent solubility of amyloid proteins, *Annu. Rev. Biochem. 66*, 385−407.
4. Lansbury, P. T. (1996) A reductionist view of Alzheimer's disease, *Acc. Chem. Res. 29*, 317−321.
5. Wood, S. J., Maleeff, B., Hart, T., and Wetzel, R. (1996) Physical, morphological and functional differences between pH 5.8 and 7.4 aggregates of the Alzheimer's amyloid peptide AP, *J. Mol. Biol. 256*, 870−877.
6. Wood, S. J., MacKenzie, L., Maleeff, B., Hurle, M. R., and Wetzel, R. (1996) Selective inhibition of A beta fibril formation, *J. Biol. Chem. 271*, 4086−4092.
7. Lambert, M. P., Barlow, A. K., Chromy, B. A., Edwards, C., Freed, R., Liosatos, M., Morgan, T. E., Rozovsky, I., Trommer, B., Viola, K. L., Wals, P., Zhang, C., Finch, C. E., Krafft, G. A., and Klein, W. L. (1998) Diffusible, nonfibrillar ligands derived from A beta-(1−42) are potent central nervous system neurotoxins, *Proc. Natl. Acad. Sci. U.S.A. 95*, 6448−6453.

8. Walsh, D. M., Hartley, D. M., Kusumoto, Y., Fezoui, Y., Condron, M. M., Lomakin, A., Benedek, G. B., Selkoe, D. J., and Teplow, D. B. (1999) Amyloid beta-protein fibrillogenesis—Structure and biological activity of protofibrillar intermediates, *J. Biol. Chem. 274*, 25945−25952.
9. Kirkitadze, M. D., Bitan, G., and Teplow, D. B. (2002) Paradigm shifts in Alzheimer's disease and other neuro degenerative disorders: The emerging role of oligomeric assemblies, *J. Neurosci. Res. 69*, 567−577.
10. Walsh, D. M., Klyubin, I., Fadeeva, J. V., Cullen, W. K., Anwyl, R., Wolfe, M. S., Rowan, M. J., and Selkoe, D. J. (2002) Naturally secreted oligomers of amyloid beta protein potently inhibit hippocampal long-term potentiation in vivo, *Nature 416*, 535−539.
11. Klein, W. L., Krafft, G. A., and Finch, C. E. (2001) Targeting small A beta oligomers: the solution to an Alzheimer's disease conundrum?, *Trends Neurosci. 24*, 219−224.
12. Hou, L. M., Shao, H. Y., Zhang, Y. B., Li, H., Menon, N. K., Neuhaus, E. B., Brewer, J. M., Byeon, I. J. L., Ray, D. G., Vitek, M. P., Iwashita, T., Makula, R. A., Przybyla, A. B., and Zagorski, M. G. (2004) Solution NMR studies of the A beta(1−40) and A beta(1−42) peptides establish that the met35 oxidation state affects the mechanism of amyloid formation, *J. Am. Chem. Soc. 126*, 1992−2005.
13. Lim, K. H. (2006) A weakly clustered N-terminus inhibits Aβ amyloidogenesis, *ChemBioChem 7*, 1662−1666.
14. Gursky, O., and Aleshkov, S. (2000) Temperature-dependent beta-sheet formation in beta-amyloid A beta(1−40) peptide in water: uncoupling beta-structure folding from aggregation, *Biochim. Biophys. Acta—Protein Struct. Mol. Enzymol. 1476*, 93−102.
15. Kusumoto, Y., Lomakin, A., Teplow, D. B., and Benedek, G. B. (1998) Temperature dependence of amyloid beta-protein fibrillization, *Proc. Natl. Aca. Sci. U.S.A. 95*, 12277−12282.
16. Bush, A. I. (2003) The metallobiology of Alzheimer's disease, *Trends Neurosci. 26*, 207−214.
17. Huang, X. D., Cuajungco, M. P., Atwood, C. S., Hartshorn, M. A., Tyndall, J. D. A., Hanson, G. R., Stokes, K. C., Leopold, M., Multhaup, G., Goldstein, L. E., Scarpa, R. C., Saunders, A. J., Lim, J., Moir, R. D., Glabe, C., Bowden, E. F., Masters, C. L., Fairlie, D. P., Tanzi, R. E., and Bush, A. I. (1999) Cu(II) potentiation of Alzheimer A beta neurotoxicity—Correlation with cell-free hydrogen peroxide production and metal reduction, *J. Biol. Chem. 274*, 37111−37116.
18. Bush, A. I., Pettingell, W. H., Multhaup, G., Paradis, M. D., Vonsattel, J. P., Gusella, J. F., Beyreuther, K., Masters, C. L., and Tanzi, R. E. (1994) Rapid induction of Alzheimer a-beta amyloid formation by zinc, *Science 265*, 1464−1467.
19. Moir, R. D., Atwood, C. S., Huang, X., Tanzi, R. E., and Bush, A. I. (1999) Mounting evidence for the involvement of zinc and copper in Alzheimer's disease, *Eur. J. Clin. Invest. 29*, 569−570.
20. Huang, X. D., Atwood, C. S., Hartshorn, M. A., Multhaup, G., Goldstein, L. E., Scarpa, R. C., Cuajungco, M. P., Gray, D. N., Lim, J., Moir, R. D., Tanzi, R. E., and Bush, A. I. (1999) The A beta peptide of Alzheimer's disease directly produces hydrogen peroxide through metal ion reduction, *Biochemistry 38*, 7609−7616.
21. Lovell, M. A., Robertson, J. D., Teesdale, W. J., Campbell, J. L., and Markesbery, W. R. (1998) Copper, iron and zinc in Alzheimer's disease senile plaques, *J. Neurol. Sci. 158*, 47−52.
22. Sparks, D. L., and Schreurs, B. G. (2003) Trace amounts of copper in water induce b-amyloid plaques and learning deficits in a rabbit model of Alzheimer's disease, *Proc. Natl. Acad. Sci. U.S.A. 100*, 11065−11069.
23. Cherny, R. A., Atwood, C. S., Xilinas, M. E., Gray, D. N., Jones, W. D., McLean, C. A., Barnham, K. J., Volitakis, I., Fraser, F. W., Kim, Y. S., Huang, X. D., Goldstein, L. E., Moir, R. D., Lim, J. T., Beyreuther, K., Zheng, H., Tanzi, R. E., Masters, C. L., and Bush, A. I. (2001) Treatment with a copper-zinc chelator markedly and rapidly inhibits beta-amyloid accumulation in Alzheimer's disease transgenic mice, *Neuron 30*, 665−676.
24. Mekmouche, Y., Coppel, Y., Hochgrafe, K., Guilloreau, L., Tallmard, C., Mazarguil, H., and Faller, P. (2005) Characterization of the Zn-II binding to the peptide amyloid-beta(1−16) linked to Alzheimer's disease, *ChemBioChem 6*, 1663−1671.
25. Miura, T., Suzuki, K., Kohata, N., and Takeuchi, H. (2000) Metal binding modes of Alzheimer's amyloid beta-peptide in insoluble aggregates and soluble complexes, *Biochemistry 39*, 7024−7031.
26. Hou, L. M., and Zagorski, M. G. (2006) NMR reveals anomalous copper(II) binding to the amyloid A beta peptide of Alzheimer's disease, *J. Am. Chem. Soc. 128*, 9260−9261.
27. Smith, D. P., Smith, D. G., Curtain, C. C., Boas, J. F., Pilbrow, J. R., Ciccotosto, G. D., Lau, T. L., Tew, D. J., Perez, K., Wade, J. D., Bush, A. I., Drew, S. C., Separovic, F., Masters, C. L., Cappai, R., and Barnham, K. J. (2006) Copper-mediated amyloid-beta toxicity is associated with an intermolecular histidine bridge, *J. Biol. Chem. 281*, 15145−15154.
28. Zirah, S., Kozin, S. A., Mazur, A. K., Blond, A., Cheminant, M., Segalas-Milazzo, I., Debey, P., and Rebuffat, S. (2006) Structural changes of region 1−16 of the Alzheimer disease amyloid beta-peptide upon zinc binding and in vitro aging, *J. Biol. Chem. 281*, 2151−2161.
29. Karr, J. W., Kaupp, L. J., and Szalai, V. A. (2004) Amyloid-beta binds Cu2+ in a mononuclear metal ion binding site, *J. Am. Chem. Soc. 126*, 13534−13538.
30. Syme, C. D., Nadal, R. C., Rigby, S. E. J., and Viles, J. H. (2004) Copper binding to the amyloid-beta (A beta) peptide associated with Alzheimer's disease—Folding, coordination geometry, pH dependence, stoichiometry, and affinity of A beta-(1−28): Insights from a range of complementary spectroscopic techniques, *J. Biol. Chem. 279*, 18169−18177.
31. Curtain, C. C., Ali, F., Volitakis, I., Cherny, R. A., Norton, R. S., Beyreuther, K., Barrow, C. J., Masters, C. L., Bush, A. I., and Barnham, K. J. (2001) Alzheimer's disease amyloid-beta binds copper and zinc to generate an allosterically ordered membrane-penetrating structure containing superoxide dismutase-like subunits, *J. Biol. Chem. 276*, 20466−20473.
32. Karr, J. W., Akintoye, H., Kaupp, L. J., and Szalai, V. A. (2005) N-terminal deletions modify the Cu^{2+} binding site in amyloid-beta, *Biochemistry 44*, 5478−5487.
33. Liu, S. T., Howlett, G., and Barrow, C. J. (1999) Histidine-13 is a crucial residue in the zinc ion-induced aggregation of the A beta peptide of Alzheimer's disease, *Biochemistry 38*, 9373−9378.
34. Zou, J., Kajita, K., and Sugimoto, N. (2001) Cu^{2+} inhibits the aggregation of amyloid beta-peptide(1−42) in vitro, *Angew. Chem., Int. Ed. 40*, 2274.
35. Yoshiike, Y., Tanemura, K., Murayama, O., Akagi, T., Murayama, M., Sato, S., Sun, X. Y., Tanaka, N., and Takashima, A. (2001) New insights on how metals disrupt amyloid beta-aggregation and their effects on amyloid-beta cytotoxicity, *J. Biol. Chem. 276*, 32293−32299.
36. Stine, W. B., Dahlgren, K. N., Krafft, G. A., and LaDu, M. J. (2003) In vitro characterization of conditions for amyloid-beta peptide oligomerization and fibrillogenesis, *J. Biol. Chem. 278*, 11612−11622.
37. Fancy, D. A., and Kodadek, T. (1999) Chemistry for the analysis of protein-protein interactions: Rapid and efficient cross-linking triggered by long wavelength light, *Proc. Natl. Acad. Sci. U.S.A. 96*, 6020−6024.
38. Bitan, G., Lomakin, A., and Teplow, D. B. (2001) Amyloid beta-protein oligomerization—Prenucleation interactions revealed by photo-induced cross-linking of unmodified proteins, *J. Biol. Chem. 276*, 35176−35184.
39. Danielsson, J., Andersson, A., Jarvet, J., and Graslund, A. (2006) N-15 relaxation study of the amyloid beta-peptide: structural propensities and persistence length, *Magn. Reson. Chem. 44*, S114−S121.
40. Syme, C. D., and Viles, J. H. (2006) Solution H-1 NMR investigation of Zn^{2+} and Cd^{2+} binding to amyloid-beta peptide (A beta) of Alzheimer's disease, *Biochim. Biophys. Acta 1764*, 246−256.
41. Danielsson, J., Pierattelli, R., Banci, L., and Graslund, A. (2007) High-resolution NMR studies of the zinc-binding site of the Alzheimer's amyloid beta-peptide, *FEBS J. 274*, 46−59.
42. Talmard, C., Guilloreau, L., Coppel, Y., Mazarguil, H., and Faller, P. (2007) Amyloid-beta peptide forms monomeric complexes with Cu-II and Zn-II prior to aggregation, *ChemBioChem 8*, 163−165.
43. Younkin, S. G. (1995) Evidence that a-Beta-42 is the real culprit in Alzheimers-disease, *Ann. Neurol. 37*, 287−288.
44. Selkoe, D. J. (1999) Translating cell biology into therapeutic advances in Alzheimer's disease, *Nature 399*, A23−A31.
45. Weggen, S., Eriksen, J. L., Das, P., Sagi, S. A., Wang, R., Pietrzik, C. U., Findlay, K. A., Smith, T. E., Murphy, M. P., Butler, T., Kang, D. E., Marquez-Sterling, N., Golde, T. E., and Koo, E. H. (2001) A subset of NSAIDs lower amyloidogenic A beta 42 independently of cyclooxygenase activity, *Nature 414*, 212−216.

46. Dahlgren, K. N., Manelli, A. M., Stine, W. B., Baker, L. K., Krafft, G. A., and LaDu, M. J. (2002) Oligomeric and fibrillar species of amyloid-beta peptides differentially affect neuronal viability, *J. Biol. Chem. 277*, 32046−32053.
47. McGowan, E., Pickford, F., Kim, J., Onstead, L., Eriksen, J., Yu, C., Skipper, L., Murphy, M. P., Beard, J., Das, P., Jansen, K., DeLucia, M., Lin, W. L., Dolios, G., Wang, R., Eckman, C. B., Dickson, D. W., Hutton, M., Hardy, J., and Golde, T. (2005) A beta 42 is essential for parenchymal and vascular amyloid deposition in mice, *Neuron 47*, 191−199.
48. Villanueva, J., Hoshino, M., Katou, H., Kardos, J., Hasegawa, K., Naiki, H., and Goto, Y. (2004) Increase in the conformational flexibility of beta(2)-microglobulin upon copper binding: A possible role for copper in dialysis-related amyloidosis, *Protein Sci. 13*, 797−809.
49. Rasia, R. M., Bertoncini, C. W., Marsh, D., Hoyer, W., Cherny, D., Zweckstetter, M., Griesinger, C., Jovin, T. M., and Fernandez, C. O. (2005) Structural characterization of copper(II) binding to alpha-synuclein: Insights into the bioinorganic chemistry of Parkinson's disease, *Proc. Natl. Acad. Sci. U.S.A. 102*, 4294−4299.
50. Sung, Y. H., Rospigliosi, C., and Eliezer, D. (2006) NMR mapping of copper binding sites in alpha-synuclein, *Biochim. Biophys. Acta 1764*, 5−12.
51. Hilbich, C., Kisters-Woike, B., Reed, J., Masters, C. L., and Beyreuther, K. (1992) Substitutions of hydrophobic amino acids reduce the amyloidogenicity of Alzheimer's disease beta A4 peptides, *J. Mol. Biol. 228*, 460−473.
52. Wood, S. J., Wetzel, R., Martin, J. D., and Hurle, M. R. (1995) Prolines and amyloidogenicity in fragments of the Alzheimer's peptide beta/A4, *Biochemistry 34*, 724−730.
53. Kirschner, D. A., Inouye, H., Duffy, L. K., Sinclair, A., Lind, M., and Selkoe, D. J. (1987) Synthetic peptide homologous to beta-protein from Alzheimer-disease forms amyloid-like fibrils in vitro, *Proc. Natl. Acad. Sci. U.S.A. 84*, 6953−6957.
54. Tracz, S. M., Abedini, A., Driscoll, M., and Raleigh, D. P. (2004) Role of aromatic interactions in amyloid formation by peptides derived from human amylin, *Biochemistry 43*, 15901−15908.
55. Bitan, G., Kirkitadze, M. D., Lomakin, A., Vollers, S. S., Benedek, G. B., and Teplow, D. B. (2003) Amyloid beta-protein (A beta) assembly: A beta 40 and A beta 42 oligomerize through distinct pathways, *Proc. Natl. Acad. Sci. U.S.A. 100*, 330−335.
56. Bitan, G., Vollers, S. S., and Teplow, D. B. (2003) Elucidation of primary structure elements controlling early amyloid beta-protein oligomerization, *J. Biol. Chem. 278*, 34882−34889.
57. Frederickson, C. J., Koh, J. Y., and Bush, A. I. (2005) The neurobiology of zinc in health and disease, *Nat. Rev. Neurosci. 6*, 449−462.
58. Maynard, C. J., Bush, A. I., Masters, C. L., Cappai, R., and Li, Q. X. (2005) Metals and amyloid-beta in Alzheimer's disease, *Int. J. Exp. Pathol. 86*, 147−159.
59. Cuajungco, M. P., Faget, K. Y., Huang, X. D., Tanzi, R. E., and Bush, A. I. (2000) *Molecular Basis of Dementia* pp 292−304.
60. Jun, S. M., and Saxena, S. (2007) The aggregated state of amyloid-beta peptide in vitro depends on Cu^{2+} ion concentration, *Angew. Chem., Int. Ed. 46*, 3959−3961.
61. Smith, D. P., Ciccotosto, G. D., Tew, D. J., Fodero-Tavoletti, M. T., Johanssen, T., Masters, C. L., Barnham, K. J., and Cappai, R. (2007) Concentration dependent Cu^{2+} induced aggregation and dityrosine formation of the Alzheimer's disease amyloid-beta peptide, *Biochemistry 46*, 2881−2891.
62. Chen, Y. R., Huang, H. B., Chyan, C. L., Shiao, M. S., Lin, T. H., and Chen, Y. C. (2006) The effect of A beta conformation on the metal affinity and aggregation mechanism studied by circular dichroism spectroscopy, *J. Biochem. 139*, 733−740.
63. Ma, Q. F., Hu, J., Wu, W. H., Liu, H. D., Du, J. T., Fu, Y., Wu, Y. W., Lei, P., Zhao, Y. F., and Li, Y. M. (2006) Characterization of copper binding to the peptide amyloid-beta(1−16) associated with Alzheimer's disease, *Biopolymers 83*, 20−31.
64. Kowalik-Jankowska, T., Ruta, M., Wisniewska, K., and Lankiewicz, L. (2003) Coordination abilities of the 1−16 and 1−28 fragments of beta-amyloid peptide towards copper(II) ions: a combined potentiometric and spectroscopic study, *J. Inorg. Biochem. 95*, 270−282.
65. Dai, X. L., Sun, Y. X., and Jiang, Z. F. (2006) Cu(II) potentiation of alzheimer A beta 1−40 cytotoxicity and transition on its secondary structure, *Acta Biochim. Biophys. Sin. 38*, 765−772.
66. Danielsson, J., Jarvet, J., Damberg, P., and Graslund, A. (2005) The Alzheimer beta-peptide shows temperature-dependent transitions between left-handed 3(1)-helix, beta-strand and random coil secondary structures, *FEBS J. 272*, 3938−3949.
67. Wolfe, M. S. (2002) Therapeutic strategies for Alzheimer's disease, *Nat. Rev. Drug Discovery 1*, 859−866.
68. Maji, S. K., Amsden, J. J., Rothschild, K. J., Condron, M. M., and Teplow, D. B. (2005) Conformational dynamics of amyloid beta-protein assembly probed using intrinsic fluorescence, *Biochemistry 44*, 13365−13376.
69. Wurth, C., Guimard, N. K., and Hecht, M. H. (2002) Mutations that reduce aggregation of the Alzheimer's A beta 42 peptide: an unbiased search for the sequence determinants of A beta amyloidogenesis, *J. Mol. Biol. 319*, 1279−1290.
70. Narayanan, S., and Reif, B. (2005) Characterization of chemical exchange between soluble and aggregated states of beta-amyloid by solution-state NMR upon variation of salt conditions, *Biochemistry 44*, 1444−1452.
71. Riek, R., Guntert, P., Dobeli, H., Wipf, B., and Wuthrich, K. (2001) NMR studies in aqueous solution fail to identify significant conformational differences between the monomeric forms of two Alzheimer peptides with widely different plaque-competence, A beta(1−40)(ox) and A beta(1−42)(ox), *Eur. J. Biochem. 268*, 5930−5936.
72. Garzon-Rodriguez, W., Vega, A., Sepulveda-Becerra, M., Milton, S., Johnson, D. A., Yatsimirsky, A. K., and Glabe, C. G. (2000) A conformation change in the carboxyl terminus of Alzheimer's A beta(1−40) accompanies the transition from dimer to fibril as revealed by fluorescence quenching analysis, *J. Biol. Chem. 275*, 22645−22649.
73. Torok, M., Milton, S., Kayed, R., Wu, P., McIntire, T., Glabe, C. G., and Langen, R. (2002) Structural and dynamic features of Alzheimer's A beta peptide in amyloid fibrils studied by site-directed spin labeling, *J. Biol. Chem. 277*, 40810−40815.
74. Petkova, A. T., Ishii, Y., Balbach, J. J., Antzutkin, O. N., Leapman, R. D., Delaglio, F., and Tycko, R. (2002) A structural model for Alzheimer's beta-amyloid fibrils based on experimental constraints from solid state NMR, *Proc. Natl. Acad. Sci. U.S.A. 99*, 16742−16747.
75. Whittemore, N. A., Mishra, R., Kheterpal, I., Williams, A. D., Wetzel, R., and Serpersu, E. H. (2005) Hydrogen-deuterium (H/D) exchange mapping of A ss(1−40) amyloid fibril secondary structure using nuclear magnetic resonance spectroscopy, *Biochemistry 44*, 4434−4441.
76. Lim, K. H., Collver, H. H., Le, Y. T. H., Nagchowdhuri, P., and Kenney, J. M. (2007) Characterizations of distinct amyloidogenic conformations of the A beta (1−40) and (1−42) peptides, *Biochem. Biophys. Res. Commun. 353*, 443−449.
77. Yan, Y. L., and Wang, C. Y. (2006) A beta 42 is more rigid than A beta 40 at the C terminus: Implications for A beta aggregation and toxicity, *J. Mol. Biol. 364*, 853−862.
78. Ahn, H., Le, Y. T. H., Nagchowdhri, P., deRose, E. E., Putnam-evans, C., London, R. E., Markley, J. L., and Lim, K. H. (2006) NMR charaterizations of an amyloidogenic conformational ensemble of the PI3K SH3 domain, *Protein Sci. 15*, 2552−2557.
79. Katou, H., Kanno, T., Hoshino, M., Hagihara, Y., Tanaka, H., Kawai, T., Hasegawa, K., Naiki, H., and Goto, Y. (2002) The role of disulfide bond in the amyloidogenic state of beta(2)-microglobulin studied by heteronuclear NMR, *Protein Sci. 11*, 2218−2229.
80. Karr, J. W., and Szalai, V. A. (2007) Role of aspartate-1 in Cu(II) binding to the amyloid-beta peptide of Alzheimer's disease, *J. Am. Chem. Soc. 129*, 3796.
81. Dong, J. J., Shokes, J. E., Scott, R. A., and Lynn, D. G. (2006) Modulating amyloid self-assembly and fibril morphology with Zn(II), *J. Am. Chem. Soc. 128*, 3540−3542.
82. Petkova, A. T., Yau, W. M., and Tycko, R. (2006) Experimental constraints on quaternary structure in Alzheimer's beta-amyloid fibrils, *Biochemistry 45*, 498−512.

BI701112Z